INFLUENCE OF HIGH LOADING RATE ON THE FRACTURE TOUGHNESS OF STEELS

G. PLUVINAGE and V. GARNIER

Laboratoire de Fiabilité Mécanique, Université de METZ, France

ABSTRACT

The fracture toughness of 3 steels was determined as a function of temperature in static and dynamic conditions. Very high loading rates ($\dot{K} \simeq 10^6$ MPa$\sqrt{m}s^{-1}$) are obtained by using stress wave loading with a split Hopkinson pressure bar apparatus. The instability of a crack in such particular conditions is examined. The amplitude of the temperature shift between the transition temperature obtained in static and dynamic conditions is compared with the results given by BARSOM's formula. The possibility to use a stress local criterion for fracture as RKR criterion, in dynamic conditions, is examined.

Conventional linear fracture toughness tests, as described in ASTM E399 standards are not able to describe plane strain fracture toughness K_{Ic} of strain rate sensitive materials. The rapid load plane strain fracture toughness property denoted by $K_{Ic}(\dot{K})$ where the loading parameter $\dot{K}$ is indicated between brackets. $\dot{K}$, the loading rate parameter characterizes the rate of evolution of stress and strain distribution at the crack tip and is given by

$$\dot{K} = K_{Ic}/t_c \qquad (1)$$

This concept cannot be confused with the velocity dependence of the dynamic fracture toughness $K_{Ic}(a)$ associated with a rapidly propagating crack. A large spectrum of $\dot{K}$ values can be explored using several kinds of testing machines quasi-static testing machines give 10^{-2}MPa m/s < $\dot{K}$ < 10^3MPa m/s ; modified close-loop testing machines extend this domain until 10^4 MPa$\sqrt{m}$/s. The well-known instrumented Charpy impact test is used

to obtain 10^4 - 10^5 Mpa$\sqrt{m}$/s $\dot{K}$ values. For higher loading rates, stress wave loadings, as Split hopkinson pressure bars (SHPB) are necessary [1] For steels, the most important effect of strain rate is to shift toughness transition temperature to higher values. BARSOM[2] has proposed an empirical relationship to calculate this temperature shift from the yield strength σ_y and the strain rate $\dot{\varepsilon}$.

$$\Delta T = (83 - 0{,}08\ \sigma_y)\dot{\varepsilon}^{\ 0{,}17} \qquad (2)$$

The effect of strain rate elevation is similar to the effect of decreasing temperature, and many authors [3-4] have tried to quantify the fracture toughness variations with temperature and strain rate with ZENER HOLLOMON parameter

$$P = T \log (A/\dot{\varepsilon}) \quad A \text{ is a frequency factor } (s^{-1}) \qquad (3)$$

The objective of this study is to evaluate the effect of high speed loading on the fracture toughness transition curve of a structural steel and the interpretation of this evolution by simultaneous examination of the influence of the loading rate on comportment law's.

I. DESCRIPTION OF THE MODIFIED SPLIT HOPKINSON PRESSURE BARS

High rates of loading ($K \simeq 2\ 10^6$ MPa$\sqrt{m}$/s) are obtained by setting the specimen between two instrumented Hopkinson bars (figure 1). Striker bar is launched from a gas gun at a desired velocity. The impact of the striker on the face of the incident bar develops a longitudinal compression wave that propagates along this bar. A wedge is attached to the incident bar and is setted in a mechanical slot of the WLCT specimen (figure 2). A part of the incident wave is reflected at the wedge-specimen contact point as a tensile pulse ε_r and a part is transmitted into the transmitter bar as a compressive pulse ε_t. These amplitude waves are registred by strain gages and digital transient recorders.

The registration of the incident ε_I, reflected ε_r and transmitted ε_T pulses provides all the information concerning specimen loading and fracturing.

It has been shown [5] that the force acting on the contact surface between the transmitter bar and specimen is given by

$$P(t) = E\ S\ \varepsilon_T(t) \qquad (4)$$

where S is the cross section of the transmitted bar, E the Young modulus of the bar's steel. It must be mentioned that the great advantage of the SHPB system lies in the dynamic calibration of elastic strains measured by strain gauges for each experiment . Application of HOOKE's law together with the elastic wave solution enables the following calibration formula

$$\varepsilon_I = \tfrac{1}{2}\ v_o/c_o\ .\ (D_s/D_B)^2 \qquad (5)$$

where v_o is the impact velocity of the stricker measured by a velocity pick up device, D_s is the diameter of the stricker, D_B denotes the diameter of the Hopkinson bars. To calibrate the system, a longitudinal pulse is sent through the bars connected together and without specimen.

The critical load P_c is generally easily detected by "pop in" value on transmitted wave diagramm as indicated in figure 4 . Time to rupture is very short (15 - 20 µs) and fracture occurs generally when the wedge is moving at constant speed. The procedure 5% "offset" is used when any pop in can not be easily detected.

In the method used, the loading is produced by an incident wave through a carbide wedge with a 45° angle. The angular slot in the sample body is 43°. This small difference gives a small contact area along the edge lines between the wedge and sample.

Consequently, the effect of friction must be taken into account and the loading tensile force is influenced by the friction coefficient µ The compliance function Y = f(a/w) was calculated by finite elements method . It is little influenced by this friction coefficient.

2. INSTABILITY OF CRACKS UNDER HIGH STRESS INTENSIFICATION RATE

During the stress wave loading of the WLCT specimen a large number of internal reflections occurs within the time interval to fracturing. This situation is shown schematically in figure 3. If Δt denotes the transit time of the elastic wave through the specimen and to the specimen length, the transit time can be calculated, as we know the elastic speed C_ℓ

$$\Delta t = \ell_o / C_\ell \qquad (6)$$

Δt is about of $2\ 10^{-6}$ µs and the loading is constituted by an adding series (10-12) of impulse loads.

The conditions for unstable crack growth under a unique impulse load is not well understood, the situation is considerably more complicated than for a slowly applied load because of the nature of the crack tip stress and the rate dependant response of the material.

Mathematical solutions for the variation of crack tip stress intensity have been obtained by several workers [6] [7] [8] for a unique impulse load. The stress intensity factor is a complicated fonction of time, it rises sharply, overshoots the equivalent static value by an appreciable amount (25-30 %) and then oscillates around the static value with decreasing amplitude (figure 5). The use of this type of function assumes that the crack motion which initiates during excursions above K_{Ic} in the oscillatory part of the crack is arrested when $K_I(t)$ is smaller than K_{Ic} and the attendant crack increment is small. This assumption, based on the fact that the crack encounters a decreasing stress singularity field during this time, requires further studying.

A minimum time for the unstable crack growing is needed. This incubation time t_o is the necessary time for the process zone to build up to a critical state. A general form for this incubation time is given by

$$C_\ell\, t_o / a^* = g\,(a/a^*) \qquad (7)$$

where a is equal to $a^* = 1/\pi\ (K_{Ic}/\sigma_o)^2$ (8). σ_o is the applied fracture stress. This formula is only valid for a crack longer than a minimum value a min given by the effective stress intensity factor (a min ≈ 0,6 a*). In dynamic loading, the critical stress pulse amplitude required to initiate the equivalent static crack can activate several cracks with a wide range of sizes simultaneously. This has been calculated by KIPP [9] and experimental verifications are given by KALTHOFF and SHOCKLEY [10].

For short cracks the characteristic oscillations drop out very early and cause only a slight perturbation and in this case suggest that the effective dynamic stress intensity factor is equal to the static value

$$K_I(\mathrm{dyn}) = K_I(\mathrm{stat})$$

For long cracks, as suggested on figure (6) due to KIPP and for $\dot{\varepsilon} = 10^3\ s^{-1}$ (this value is very close to those obtained with the SPHB device), the effective stress intensity factor K^{eff} (dyn) is about 2/3 of the static value.

In the case of stress wave loading by the SHPB, the following experimental conditions are observed :

- The number of elastic waves reflections occuring in the specimen during time to fracturing $n = t_f/\Delta t_s$ is approximately of 10-12 and consequently the loading is constituted by a series of impulse loads.
- The stress intensity factor $K_I(t)$ is in the oscillatory part, slightly damping of the curve $K_I = f(t)$ because non dimensionnal time to rupture is sufficiently long.
- The crack length of the specimen is equivalent to a short crack $a = 1/12\ C_\ell\, t_f$.
- The strain rate at a point on the elastic plastic boundary can be calculated by the SHOEMAKER's formula [11]

$$\varepsilon = \sigma_y / E \times \dot{K}/K \qquad (9)$$

is about $10^3\ s^{-1}$. For this value, the strain rate sensitivity of the material is only governed by the thermal activation and the yield stress is a logarithmic function of the strain rate. The elasto-plastic behaviour law can be used for modelization. These remarks lead to use, in this particular case ($K < 2\text{-}3\ 10^6$ MPa√m/s, $a < 1/10\ C_\ell\, t_f$) the quasi-static solution for stress intensity factor for brittle materials loaded by stress waves with the Split Hopkinson Pressure Bar.

3. MATERIALS AND RESULTS

Tests have been performed on 3 steels

materials	yield strength $\dot{\varepsilon} = 10^{-3}\ s^{-1}$
Steel XC38	σ_y = 400 MPa
Steel XC28Ar	σ_y = 650 MPa
Steel 35NCDV12	σ_y = 1315 MPa

The chemical composition is only known for XC38 and 35NCDV12 steel

	C	Si	Mn	P	S	Cr	Ni	Mo
XC38	0,38	0,25	0,55	0,025	0,025	-	-	-
35NCDV12	0,36	0,289	0,81	0,09	0,003	15,72	4,24	1,02

The static and dynamic fracture toughness is plotted as a function of test temperature for the 3 steels considered in this study (figure 7). The results that are only presented are valid according to the ASTM E 399 procedure, in particular plane strain condition given by :

$$(W - a) \text{ or } B > 2{,}5 \left(K_{Ic}/\sigma_y\right)^2 \qquad (10)$$

Technological limitations were imposed for the building of the SHPB, bars have a diameter of 20 mm and consequently maximal thickness of the specimen according to a good transmission of stress waves is 20 mm.

For this reason the static and dynamic fracture toughness is limited to the foot of brittle ductile transition defined at K_{Ic} (transition) = 70 MPa$\sqrt{m}$.

In each case increasing the strain rate causes the fracture toughness to decrease and a shift of the fracture toughness curves ΔT defined as :

$$\Delta T = T^{70\ MPa\sqrt{m}}_{K_{Ic}(1)} - T^{70\ MPa\sqrt{m}}_{K_{Ic}(10^6)} \qquad (11)$$

The results for the three materials and a comparison with the Barsom's formula are given in Table 1

Steel	ΔT calculated	ΔT experimental
XC38	165°C	150°C
XC28	100°C	110°C
35NCDV12	impossible	31°C

TABLE 1

Some remarks are made on the Barsom's formula

$$\Delta T = (83 - 0{,}08\ \sigma_y)\dot{\varepsilon}^{\,0{,}17} \qquad (12)$$

- In this formula ΔT is given in Celsius'Degree, σ_y in MPa and $\dot{\varepsilon}$ calculated by SHOEMAKER formula in s^{-1}.

- This value of $\dot{\varepsilon}$ is not the maximum or the average strain rate value.

- The Barsom's formula has been established for the maximum strain rate given by instrumented charpy impact tests (10^2 - 5 10^2 s^{-1}) and for low and medium strength steels (σ_y < 965 MPa).

These results show that for steels with a yield stress below 1000 MPa, this formula gives satisfactory results. This is according to recent works of MARANDET, PHELIPPEAU and SANZ [12].

Until value of $\dot{\varepsilon}$ = 2 $10^3 s^{-1}$ plastic flow is governed by the thermally activated motion of dislocations, and yield strength is a function of an activation energy ΔG, which is related to a strain rate by an Arrhenius equation

$$\dot{\varepsilon} = B \exp \Delta G(\sigma)/KT \qquad (13)$$

where $\dot{\varepsilon}$ is the strain rate , B is a constant depending on the material $\Delta G(\sigma)$ activation energy, K is the Bolzmann constant and T the temperature in ° K.

An other convenient way to represent this phenomenon is the use of the Zener Hollomon parameter

$$P = T \log (A/\dot{\varepsilon}) \qquad (14)$$

where A is a frequency factor. This parameter has been used by several authors [12-13-14] in order to represent by a unique curve the influence of strain rate and temperature. All data evaluated over a wide range of different temperatures and 2 different strain rates fit on single curve with a small scatterband (figure 8).

The frequency factor is 10^{13} for XC28Ar steel, 10^{16} for XC38 steel and 10^{45} for 35NCDV12 steel.

4. RELATION BETWEEN COMPORTMENT LAW AND FRACTURE TOUGHNESS EVOLUTIONS AT HIGH STRAIN RATE

In order to explain the temperature shift of fracture toughness curve at high strain rate, a particular attention has been given to determine the relation between uniaxial flow properties versus the strain rate and the fracture toughness $K_{Ic}(\dot{K})$. Other phenomena as crack tip heating and the modification of rupture process seem not to be influent enough [1] to explain the modification of fracture toughness at this level of high strain rate. The value of K_{Ic} can be calculated with the help of a critical stress criterion [15] [16].

The influence of strain rate and temperature on yield strength is schematically given on figure 9 . The domain I is characterized by a low influence of strain rate and temperature on yield strength; plasticity has an athermal character. In the domain II, the influence of $\dot{\varepsilon}$ and T is very important, dislocation movement is governed by thermal activation. The zone III, at very low temperature is characterized by a very little influence. In zone IV, yield strength is very sensitive to very high strain rate $\dot{\varepsilon} = 10^3 - 10^6\ s^{-1}$. The same split Hopkinson pressure bar can be used to obtain comportment law $\sigma = f(\varepsilon, \dot{\varepsilon})$ for $\dot{\varepsilon} = 10^3\ s^{-1}$). The specimen used are small cylinders of 10 mm of diameter and 5 mm high and are inserted between incident and transmitted bars. During tests the continuous strain time histories of the incident $\varepsilon_I(t)$, reflected $\varepsilon_r(t)$ and transmitted $\varepsilon_T(t)$ waves are picked up by the strain gauge stations and it is possible to determine complete stress strain characteristics of the specimen material. Further it is possible to obtain

$$\begin{aligned} &\text{the strain history} && \varepsilon(t) = 2C_\ell/\ell_o \int_o^t \varepsilon_r(\alpha)d\alpha \quad C_\ell \\ &\text{the strain rate} && \dot{\varepsilon} = 2\,C_\ell/\ell_o\,(\varepsilon_{r(t)}) \\ &\text{the stress history} && \sigma(t) = E(D_y/D_s)^2\,\varepsilon_T(t) \end{aligned} \qquad (15)$$

E is the Young's modulus and α a time dependent additional variable. The same specimens are used to obtain quasi-static stress-strain curves. The influence of strain rate at room temperature is given in table II

Steel	$\dot{\varepsilon} = 10^{-3}s^{-1}$	$\dot{\varepsilon} = 10^{3}s^{-1}$
XC38	400 MPa	805 MPa
XC28	650 MPa	1200 MPa
35NCDV12	1315 MPa	2480 MPa

TABLE II

A comparison with static and dynamic stress strain curves (figure 10) shows that the yield strength increases considerably (about 2 times) and plastic instability appears at high strain rate.

Yield strength σ_y is found to be a function of activation energy

$$\sigma_y = f(KT \ln B/\dot{\varepsilon}) \qquad (16)$$

The fracture toughness can be assessed in terms of local criteria in conjunction with stress-strain distribution.

This stress-strain distribution can be obtained by the well-known HRR solution for a material which obeys the stress strain law written as

$$\varepsilon_p = \gamma(\sigma/\sigma_y)^{N-1}\sigma/E \qquad (17)$$

where γ is a constant depending of the material or by finite element method - see figure 11.

The stress field is characterized by a steep gradient, when the distance from the crack tip is small. This stress field has a doubtful physical meaning when the distance to the crack tip is smaller than a characteristic distance. This characteristic distance X_o, which may be thought of as describing the minimum volume of material in which the cleavage fracture process can operate, is usually about a few grain diameter.

RITCHIE, KNOTT and RICE [15] have shown that a cleavage crack propagates in an unstable manner when the maximum principal stress ahead of the crack tip exceeds the cleavage stress σ_c and relate the fracture toughness of ferritic steels to these parameters

$$K_{Ic} = \beta\,\frac{(N+1)}{2}\,X_o^{1/2}\,\frac{\sigma_c^{\frac{N+1}{2}}}{\sigma_y^{\frac{N-1}{2}}} \qquad (18)$$

In this model it is assumed that the critical cleavage stress σ_c and the critical distance X_o are independent of the strain rate and temperature and that the work hardening parameters (β, N) are also not affected by $\dot{\varepsilon}$ and T.

The cleavage stress is generally obtained by using a axisymmetric specimen or static charpy V bend tests.

However the value calculated for this blunt notch case is lower that the true cleavage stress and must be corrected. The highly stressed volume ahead a blunt notch is larger than in front of crack. Therefore the probability of funding the weakest link is higher in the case of a blunt notch than in the case of a crack.

It seems that the cleavage stress is practically independent of the temperature (KOTILAINEN [17]) but the assumptions of the non-influence of strain have never been verified and a controversy assumption has been issued by WILSHAW [18].

The characteristic distance X_o is temperature dependent and a large scatter band of values (1 to 10 grain size for the same steel) can be found. From a physical point of view it is probably more realistic to assume that below a certain characteristic distance (1 or 2 grain size) the stress gradient is lower than one derived from calculation. The strain hardening exponent is temperature sensitive and plastic instability provides scattering in data. An experimental relation ship can be roughly found.

$$K_{Ic} \cdot \sigma_y^{\,m} = cst \qquad (19)$$

The preceeding discussion ignores the three dimensional nature of the fracture process and the "weakest link hypothesis" which derived from the Weibull theory of brittle fracture may be probably non applicable. Particularly at high strain rate, fractographic investigations indicated the possible occurence of isolated cleavage microcracks at different points along the crack front before final fracture; the occurence of these microcracks indicates that the macroscopic fracture criterion may be the attainment of the mean toughness along the crack front.

CONCLUSIONS

By using the Split Hopkinson Pressure Bars it is possible to determine dynamic fracture toughness for high strain intensification rate $\dot{K} = 10^6$ MPa$\sqrt{m}$/s. For the three structural steels investigated, it was established that an increase in the loading rate results in a decrease in the toughness when fracture occurs by cleavage.

The amplitude of the temperature shift between static and dynamic toughness transition curves was compared with the predictions given by the Barsom's formula. It appears that the Barsom's formula can be extended for high strain rate ($\dot{\varepsilon} = 10^3$) with a correction for high strength steels (σ_y > 1000 MPa).

For each steel it is possible to relate the effect of temperature and strain rate on fracture toughness by using the Zener-Hollomon parameter with a frequency factor depending on the material. In order to apply a local cleavage fracture criterion as the one proposed by RITCHIE, KNOTT and RICE, the influence of strain rate on temperature on cleavage stress, critical distance and strain hardening exponent must be also taken into consideration.

REFERENCES

[1] PLUVINAGE, G., "Mesure de la ténacité des matériaux sous sollicitations dynamiques", Colloque A.T.S., TARBES, France (1980).

[2] BARSOM, J.M., "Effect of temperature and rate loading on the fracture behaviour of various steels", Proceedings International Conference on Dynamic Fracture Toughness, Welding Institute and American Society for Metals, LONDON (July 1976) 281-302.

[3] CORTEN, H.T., and SHOEMAKER, A.V., Transaction of American Society of Mechanical Engineers, Journal of Basic Engineering (March 1967) 86-92.

[4] KRABIEL, A., and DAHL, W., "Influence of strain rate and temperature on the tensile fracture properties of structural steels", Proceedings ICF5, CANNES, France (1981) 393-400.

[5] ANDRZEJEWSKI, A., KLEPACZKO, J., and PLUVINAGE, G., "Détermination

expérimentale de la ténacité à grande vitesse de chargement d'alliages d'aluminium", Journal de Mécanique Appliquée, vol. 5, N°3 (1981) 345-366.

[6] EMBLEY, G.T., and SIH, G.C., "Response of a penny-shaped crack to impact waves", Proceedings of 12th Midwestern Mechanics Conference, 6, 473 (1981)

[7] PENSER, T., and GROSS, D., "Stress intensity factors of plane dynamic problems", Report Technische Hochschule, DARMSTADT (1981).

[8] VARDAR, O., and FINNIE, I., "The prediction of fracture in brittle solids subjected to very short duration tensile stresses", Int. Journal of Fracture (1977) 9-115.

[9] KIPP, M.E., GRADY, D.E., CHEN, E.P., "Strain rate dependent fracture initiation", International Journal of Fracture (1980) 471 478.

[10] KALTHOFF, J.F., and SHOCKEY, D.A., "Instability of cracks under impulse load", Journal of Applied Physics, vol. 48, N°3 (March 1977).

[11] SHOEMAKER, A.K., Transactions, American Society of Mechanical Engineers, Journal of Basic Engineering (Sept. 1965) 506-511.

[12] MARANDET, B , PHELIPPEAU, G., and SANZ, G., "Influence of loading rate on the fracture toughness of some structural steels", Rapport IRSID RE 908 (juillet 1982).

[13] CORTEN, H.T., and SHOEMAKER, A.K., Transaction American Society of Mechanical Engineers, Journal of basic Engineering (March 1967) 86-92.

[14] RITCHIE, R.O., KNOTT, J.F., and RICE, J.R., "On the relationship between critical tensile stress and fracture toughness in mild steel", Journal of Mech. Physic Solids, 21 (1973) 395 410.

[15] HOLLZMANN, M., VLACK, B., and BILEK, Z., "The effect of microstructure on the fracture toughness of structurals steels", Int. J. Pressure Piping, 9 (1981) 1-9.

[16] KOTILAINEN, H., Fatigue and Fracture, Ed. J. Radon, Pergamon Press OXFORD (1980) 217.

[17] WILSHAW, J.R., and PRATT, P.L., J. Mech. Physic Solids, 14 (1966) 191 211.

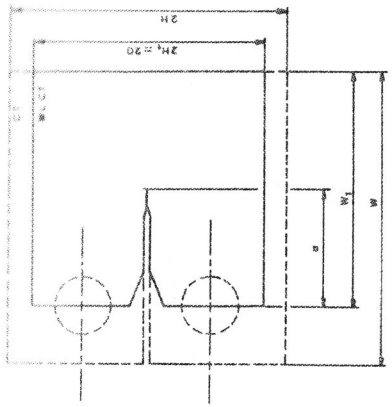

Figure 2 : Geometry of the WLCT sample

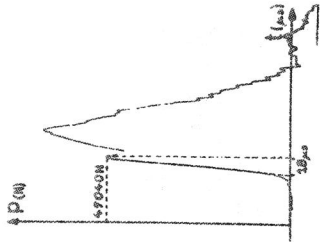

Figure 4 : Transmitted wave diagram

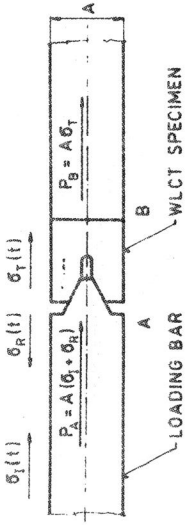

Figure 1 : Schematic experimental set up

Figure 3

Elastic Waves travelly through specimen inserted between two Hopkinson pressure bars

Δt_s specimen transit time

t_f time to fracture

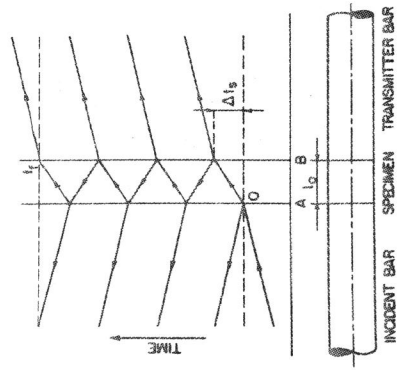

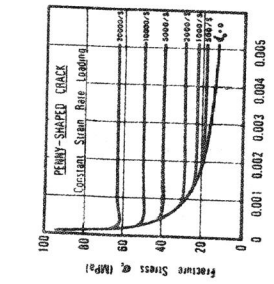

Figure 6 : Fracture stress for constant strain rate loading (KIPP et al. 1979)

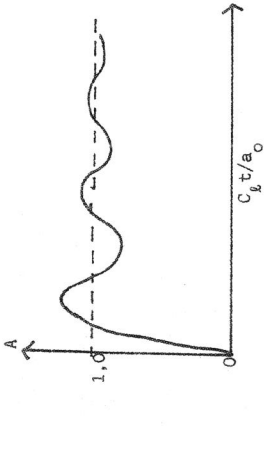

Figure 5 : Variation of the function K(dyn)/K(stat) with time for a crack load by a step wave (schematic)

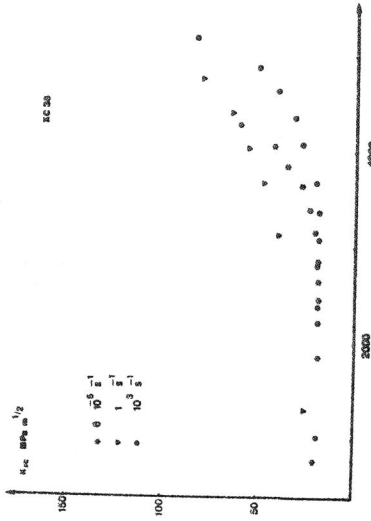

Figure 8 : Fracture toughness versus Zener Hollomon parameter for a XC38 steel

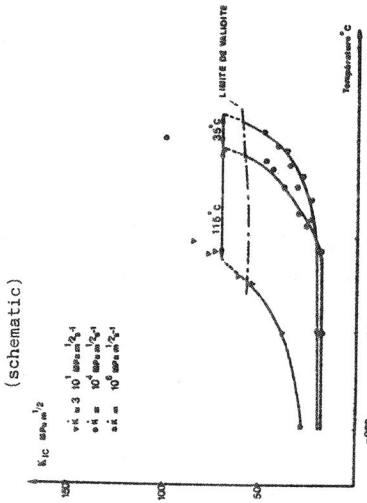

Figure 7 : Fracture toughness transition curve for XC38 steel

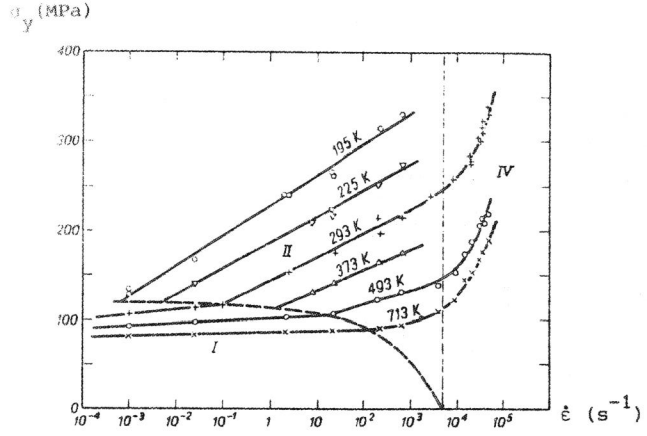

Figure 9 : Influence of strain rate and temperature on yield strength

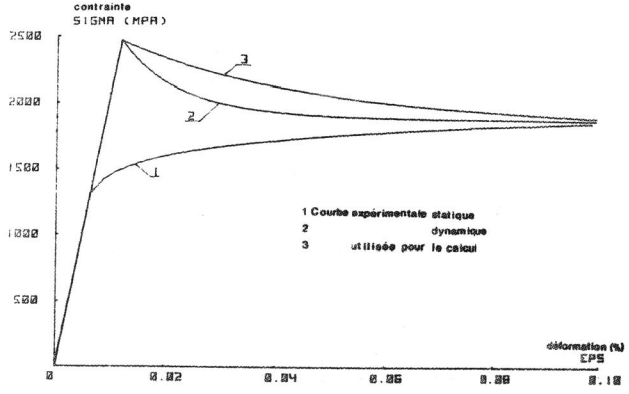

Figure 10 : Static and dynamic stress-strain curve of 35NCDV12 steel

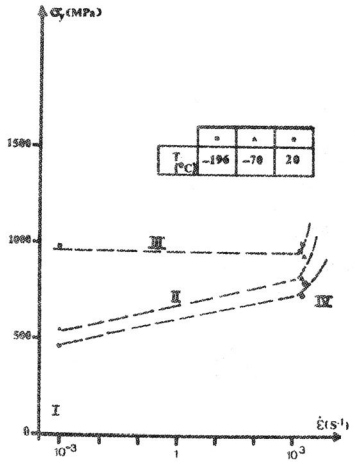

Figure 11 : Fracture toughness versus yield strength for different temperatures and strain rate for a XC38 steel

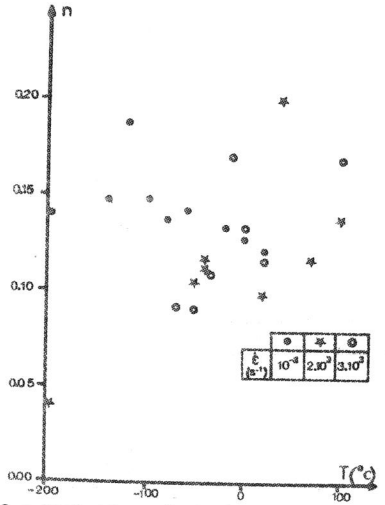

Figure 12 : Evolution of static and dynamic strain hardening exponent with temperature for a structural steel